INTERNATIONAL JOURNAL OF AGRICULTURE & BIOLOGY
ISSN Print: 1560–8530; ISSN Online: 1814–9596
20–0590/2020/24–5–1196–1206
DOI: 10.17957/IJAB/15.1549
http://www.fspublishers.org

Full Length Article

Identification, Subcellular Localization and Expression Analysis of the RgMATEs Potentially Involved in Phenolics Release in *Rehmannia glutinosa*

Yan Hui Yang[1*], Heng Yang[1], Ming Jie Li[2], Zhong Yi Zhang[2], Yan Jie Yi[1], Rui Fang Li[1], Chen Dong[1] and Chao Jie Wang[1]

[1]*College of Bioengineering, Henan University of Technology, Lianhua Street 100, Zhengzhou High-technology Zero, Henan Province, China, 450001*

[2]*College of Crop Sciences, Fujian Agriculture and Forestry University, Jinshan Road, Cangshan District, Fuzhou, China, 350002*

[*]For correspondence: yyhui2004@126.com

Received 13 April 2020; Accepted 11 June 2020; Published 31 August 2020

Abstract

The continuous cultivation of *Rehmannia glutinosa* is problematic due to its release of auto toxic allelochemicals into the rhizosphere. Phenolics have been implicated as potential agents of this autotoxicity in *R. glutinosa*. Although Multidrug and Toxic Compound Extrusion Transporters (MATEs) are known to mediate the release of certain toxins in some plants, the identification of MATEs, which contribute to the release of phenolics, which have not been explored in *R. glutinosa*. Here, we scanned *R. glutinosa* transcriptome sequences and identified 66 RgMATE transcripts. An *in silico* analysis of the RgMATEs identified 9-12 transmembrane domains which predicted that most of them were deposited on plasma membrane and function as transporters. The phylogeny and homology analysis implied that ten of the RgMATEs were potentially associated with the release of phenolics. The transient expression showed that RgMATE33 and RgMATE46 were both localized in plasma membrane. Positive correlations were established between the expression abundance of eight *RgMATE* candidate genes in hairy roots and total phenolics content in their exudation. The conclusion was that the eight RgMATE efflux transporters likely contributed to the release of phenolics into *R. glutinosa* rhizosphere. Our study will lay the foundation for revealing the molecular basis of autotoxicity formation.

Keywords: *Rehmannia glutinosa*; Phenolics release; MATE transporter; Subcellular localization; Expression analysis

Introduction

The perennial herbaceous species *Rehmannia glutinosa* Libosch belongs to the family *Orobanchaceae*. It is cultivated for its tuberous roots which contain a number of pharmacologically active compounds (Li *et al.* 2015; 2017). When replanted, the crop suffers a decline in productivity due to the release into the soil by the previous crop of autotoxic allelochemicals from some secondary metabolites (Li *et al.* 2012; Li *et al.* 2017; Zhang *et al.* 2016; 2018), a phenomenon referred to as "allelopathic autotoxicity". A similar syndrome has been documented in a number of other crop species (Tian *et al.* 2016; Li *et al.* 2020). A large number of secondary metabolites have been implicated as potential agents of these allelochemicals (Ren *et al.* 2015; Kim *et al*. 2020; Li *et al*. 2020); in *R. glutinosa*, the most likely candidates are phenolics (Li *et al.* 2012; Wu *et al*. 2015). The molecular basis of their release accumulation from the *R. glutinosa* roots remains obscure.

Multidrug and Toxic Compound extrusion Transporters (MATEs) are found in all life forms (Moriyama *et al*. 2008; Xu *et al*. 2019), and are particularly abundant in plants (Wang *et al*. 2017a; Jagessar *et al*. 2020). Plant MATEs typically fall within the size range 400–550 residues, and feature 9–12 transmembrane helical structures which function to bind their substrate (Omote *et al*. 2006; Miyauchi *et al*. 2017; Jagessar *et al.* 2020). The number of MATE-encoding genes harbored by the genomes of *Arabidopsis*, rice, tomato, blueberry, barrel medic, soybean and cotton is 56, 45, 67, 33, 70, 117 and 70 (Chen *et al.* 2015; Liu *et al.* 2016; Wang *et al*. 2016; 2017a; Santos *et al*. 2017; Xu *et al*. 2019); a set of 66,906 unigenes represented in an assembled *R. glutinosa* transcriptome has been estimated to be Li *et al.* (2017). MATEs have been implicated either directly or indirectly in the transport and accumulation of numerous phenolics release, as well as in the detoxification of autotoxins, in plant nutrient homeostasis, in tolerance to stress and in disease resistance

To cite this paper: Yang YH, H Yang, MJ Li, ZY Zhang, YJ Yi, RF Li, C Dong, CJ Wang (2020). Identification, subcellular localization and expression analysis of the RgMATEs potentially involved in phenolics release in *Rehmannia glutinosa*. *Intl J Agric Biol* 24:1196–1206

(Bashir *et al*. 2011; Ishimaru *et al*. 2011; Chen *et al*. 2015; Ma *et al*. 2018; Wang *et al*. 2020).

A strong correlation has been established between MATE activity and the transport of phenolics across a number of plant species (Ishimaru *et al*. 2011; Chen *et al*. 2015; Xu *et al*. 2019), which supports the idea that MATEs contribute significantly to this activity (Bashir *et al*. 2011; Tiwari *et al*. 2014). In *Arabidopsis thaliana*, several AtMATEs (such as AtDTX24, AtDTX25, AtDTX35 and AtDTX41/AtTT12) were associated with the transport of phenolics (Zhao and Dixon 2009; Thompson *et al*. 2010; Santos *et al*. 2017). In rice, two OsMATEs (OsPEZ1 and OsPEZ2) were demonstrated to be vital roles in phenolics release of plant roots (Ishimaru *et al*. 2011; Bashir *et al*. 2011). However, MATE transcripts, which contribute to the release of phenolics, have not yet been identified in *R. glutinosa*. To identify MATE candidate genes involved in the release of phenolics in *R. glutinosa*, the present study scanned *R. glutinosa* transcriptome sequences and explored a set of RgMATE transcripts. Base on *in silico* analysis and experimental validation, we found some RgMATE efflux transporters potentially involved in the release of phenolics to lay a foundation for elaborating the regulation of the release and accumulation of allelopathic autotoxins in *R. glutinosa*.

Materials and Methods

Identification of MATE sequences

The *in silico* identification of putative *R. glutinosa MATE* sequences was based on sequence data archived at www.ncbi.nlm.nih.gov/sra. According to Li *et al*. (2017), the transcriptome resolved into 66,906 unigenes. The transporter classification database (www.tcdb.org) was used to identify membrane transport proteins among the products encoded by these *R. glutinosa* unigenes, using the tBLASTX algorithm with the e-value set to e-3 (Saier *et al*. 2016). Their predicted translation products were scanned for the characteristic features of plant MATEs, namely the presence of ~12 transmembrane domains and a length of ~500 residues, and were retained only where their level of sequence similarity to known plant MATEs was above 30%. The TMHMM Server v.2.0 program (www.cbs.dtu.dk/services/TMHMM) was applied as a further filter. The molecular weight and predicted pI of each putative RgMATE was obtained using the ProtParam tool (web.expasy.org/protparam) and their subcellular localization was predicted using the PSORT program (https://www.psort.org) program. Blast2GO software (www.blast2go.com/) was used for allocating functionality.

Phylogenetic analysis

The phylogeny of the RgMATEs was inferred using the Neighbor-joining method implemented in the MEGA v7.0 package, applying 1,000 bootstrap replicates and based on the JTT matrix-based model (Kumar *et al*. 2016). A multiple sequence alignment of the predicted polypeptide sequences was performed using DNAMAN v6.0 software.

Transient expression for subcellular localization

For the experimental materials, *R. glutinosa* cultivar "Wen 85-5" which was provided by Wen Agricultural Institute (Jiaozuo, Henan Province, Chian) and identified *R. glutinosa* Libosch belongs to the family *Orobanchaceae* by Professor Yan Hui Yang at Henan University of Technology, China. *R. glutinosa* was cultured at the pots in a greenhouse (a constant temperature of 26°C with a 14-h-light/10-h-dark cycle) from College of Bioengineering, Henan University of Technology. The roots from five *R. glutinos*a plants were sampled after 90 culture days. Total RNA was isolated from the sampled roots using the TRIzol reagent (Invitrogen, Carlsbad, USA) as recommended by the manufacturer. A 2 µg aliquot of total RNA was reverse-transcribed in a 20 µL reaction containing 5U M-MLV reverse transcriptase (Takara, Tokyo, Japan), formulated according to the manufacturer's instructions.

To isolate the full open-reading frame (ORF) *RgMATE* genes, the primers extending from the upstream "ATG" start codon site to the downstream region including the stop codon of the gene were designed by using Oligo7.0 software (Table 1). The *RgMATE* sequences were amplified the cDNA of the samples by PCR using PrimeSTAR® HS DNA Polymerase (Takara, Tokyo, Japan). The products were purified with the TaKaRa MiniBEST Agarose Gel DNA Extraction Kit and subcloned into the pMD-18 vector (Takara, Tokyo, Japan), which was then used to transform *E. coli*. All constructs were verified by sequencing (Sangon, Shanghai, China).

For the subcellular localization of *RgMATE*, the ORF of the *RgMATE33 and RgMATE46* sequences was inserted into the pBI121 vector (Biovector Science Lab, China) under the control of the CaMV35S promoter, fused with the N-terminus of the GFP gene, to generate the CaMV35S:GFP-RgMATE constructs. The resulting constructs were transformed with the *Agrobacterium tumefaciens* GV3101 strain using the freeze-thaw method (Wise *et al*. 2006). For the transient expression of CaMV35S:RgMATE-GFP constructs in onion, the GV3101 strain, which was transformed into the CaMV35S:RgMATE-GFP constructs (an empty vector CaMV35S:GFP as control), was cultured for collection and then infiltrated into onion epidermal cells. The transfected epidermal regions were examined after 48 h of coculture. The transfected epidermal regions were analyzed with a fluorescence microscope (FV1000 MPE, Olympus) at an excitation wavelength of 488 nm to visualize GFP fluorescence.

Hairy root culture of *R. glutinosa*

Hairy roots of *R. glutinosa* were cultured under sterile

conditions up to the 20-day in 100 ml Erlenmeyer flasks containing 50 mL of MS (Murashige and Skoog 1962) liquid nutrient medium and 30 $g \cdot L^{-1}$ sucrose; the plants were exposed to a dark period and a constant temperature of 26°C (Wang *et al*. 2017b). They were subsequently transferred into fresh tubes containing 150 mL of the same liquid nutrient medium at the same cultured-condition. These roots and their nutrient medium exudation for further analysis were collected at 5, 10, 15, 20, 25, 30, 35, 40 and 45 days after transplant (DAT), respectively.

Total phenolics content assay

To estimate total phenolics content of the exudation, 150 mL from each nutrient medium of hairy roots was passed through a 0.45 μm filter and lyophilized, the residues were dissolved in 5 mL methanol. Total phenolic content was measured using the Folin–Ciocalteu method as described previously by Bursal and Gülçin (2011). Gallic acid (1–100 $\mu g \cdot mL^{-1}$) solution was used to draw a standard curve. Total phenolic content from hairy root exudation was expressed as micrograms gallic acid equivalent per milliliter of liquid nutrient medium ($\mu g \cdot GAE \cdot mL^{-1}$). Evaluation of all samples was performed with at least three biological replicates.

RNA extraction and qRT-PCR analysis

Total RNA of each hairy root samples was isolated and reverse-transcribed as the above methods mentioned. For qRT-PCR analysis, the gene primer sequences (Table 1) were designed using Beacon Designer v8.0 software (www.premierbiosoft.com) and a fragment of *R. glutinosa Actin* (Genebank ID: EU526396.1) was used as the reference sequence. Each 25 μL quantitative real-time PCR (qRT-PCR) contained 0.2 μM of forward and reverse primer, 12.5μL SYBR® Premix EX Taq™ (Takara) and 100 ng cDNA. Negative control reactions contained no cDNA. The PCR regime comprised an initial denaturing step (95°C/10 s), followed by 40 cycles of 95°C/5 s, 60°C/10 s, 72°C/15 s and a final ramping of 60–95°C to determine the amplicon's dissociation behavior. Three biological replicates were included per sample. The $2^{-\triangle\triangle CT}$ method (Livak and Schmittgen 2001) was applied to estimate relative transcript abundances and the data were normalized on the basis of the abundance of the reference gene transcript.

Statistical analyses

Error analysis for the indices (i.e., total phenolics content of the exudation and the expression abundance of *RgMATEs*) was performed applying SPSS 20.0 program. To assess the correlation on the expression abundance of *RgMATEs* from the roots and total phenolics accmulation from their exudation, we used to Pearson correlation method ($p<0.01$) of two individual variables by SPSS 20.0 program.

Results

Identification of MATE transporters

The scan of the *R. glutinosa* transcriptome revealed a set of 66 unigenes putatively encoding MATE transporters, which were deposited in NCBI Genbank (Accession numbers assigned MK120913 through MK120978), designated *RgMATE1* through *66*. The size of the predicted translation products of these sequences varied from 470 to 584 residues; their predicted molecular mass ranged from 50.56 to 62.64 kDa, their predicted pI from 4.98 to 8.19, their grand average of hydropathicity (GRAVY) from 0.39 to 0.83, their aliphatic index from 107.65 to 123.64 and the number of transmembrane domains present from nine to twelve (Table 2). All of these predicted polypeptides were likely stable because in no case was the instability index below 40. Based on *in silico* localization analysis, of the proteins, 62 were predicted to localize to the plasma membrane, two to the vacuolar membrane and one each to the endoplasmic reticulum and the nucleus.

RgMATE function according to GO analysis

The Blast2GO output for the set of RgMATEs is illustrated in Fig. 1. In terms of cellular component, the proteins were distributed between “membrane”, “membrane part”, “cell”, “cell part”, “organelle” and “organelle part”. With respect to molecular function, all were classified as being involved in transporter activity - either “drug transmembrane transporter activity” or “antiporter activity”; finally, with respect to biological process, the GO terms “localization”, “response to stimulus”, “single organism response” and “biological regulation” were represented.

MATE protein phylogeny

A phylogenetic analysis compared the sequences of the 66 RgMATEs with 56 encoded by *A. thaliana* and 30 encoded by other plants (Fig. 2). Four primary clades (C1 through C4) were recognized. The largest of these was C1 (89 sequences), which was divided into the four secondary clades C1-1 (47 sequences), -2 (23 sequences), -3 (12 sequences) and -4 (seven sequences). The C2, C3 and C4 clades harbored, respectively, 32, 21 and 20 sequences, respectively. Several MATEs involved in phenolics transportation (e.g. AtDTX41/AtTT12, AtDTX35, OsPEZ1 and OsPEZ2) were mostly classfied in C1 subfamily, thus the 49 RgMATEs belonging to subfamily were further analyzed.

Conservation of the RgMATE sequences potentially involved in phenolics transportation

Among 49 RgMATEs from C1 subfamily, we removed the RgMATE6 localized in the vacuolar membrane to remain the 48 RgMATEs localized in the plasma membrane.

Table 1: Primer sequences used for the *RgMATE* genes

Primer type	RgMATE ID	Product Length	Forward (5'→3')	Reverse (5'→3')
RgMATE-GFP constructs	RgMATE33	1871	ATGGGGTCCTTACAAAACCAAGGGGTG	GGACAATAAAGTAACAGGTATCTTGTGC
	RgMATE46	1742	ATGGAGGACAACTCCAAGCAGCCAC	CAGTCACAACATACGGAATCAACCC
qRT-PCR	RgMATE7	130	AAGATGAGGAGAAGGATT	CTGCCATAAGTGTAAGAG
	RgMATE19	128	CAATAAGCGTAAGAGTGT	GAAGATAAGTAGAGCAATAGA
	RgMATE30	90	GGTGGACGATGATGTTAT	TTGCTGTTCTTGGATGTA
	RgMATE33	168	AATACTACATGCTCGGAATA	GGATTGGCTTGGAGAATA
	RgMATE35	93	CGTGAATATAGGTTGTTA	CAGATTAAGATGAGAGTT
	RgMATE36	165	ATTGCTTGTGCTCCATAA	AGTAGAGATTGAGTGTGAAC
	RgMATE45	126	ATTCTACACGCCTACTAA	CTTCTTCTTCTTCCTCTTC
	RgMATE46	126	ATTCTACACGCCTACTAA	CTTCTTCTTCTTCCTCTTC
	RgMATE55	128	GAAGATAAGTAGAGCAATAGA	CAATAAGCGTAAGAGTGT
	RgMATE56	98	CTATCAGCGTAAGAGTGT	GCCAATTAAGAAGGAAGAT
	RgActin	235	TTCAGGCTGTCCTTTCACTG	TGCAACATATGCAAGCTTCT

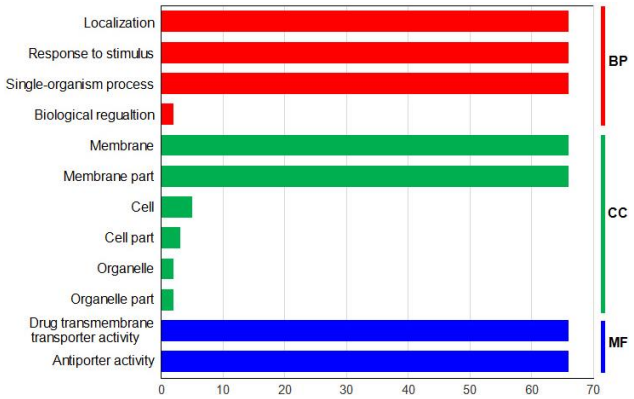

Fig. 1: Gene ontology analysis of the set of 66 *RgMATEs*. BP: Biological process; CC: Cellular component; MF: Molecular function

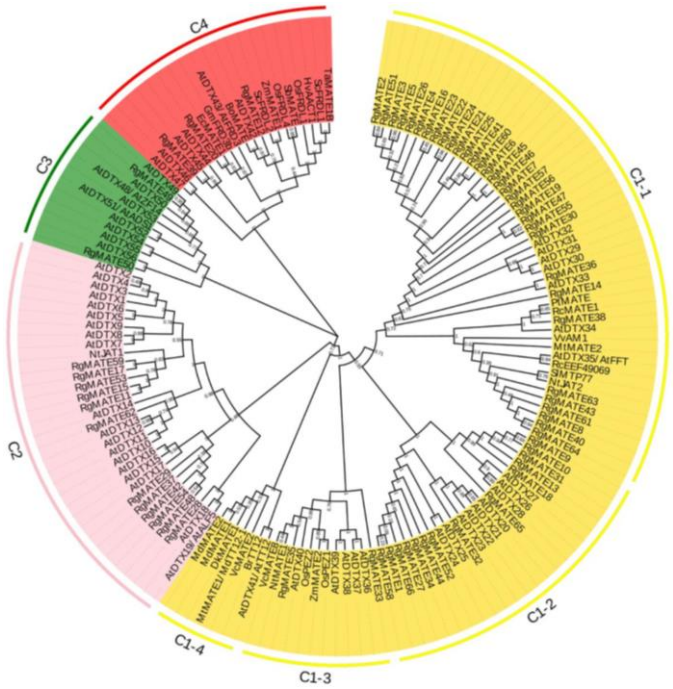

Fig. 2: Phylogeny of the set of RgMATEs, including 56 MATE homologs encoded by *A. thaliana* and 30 encoded by other plant species

A multiple sequence alignment involving the 48 RgMATEs and four heterologous MATEs associated with the efflux transport of phenolics suggested that there were 10 RgMATEs which shared at least 40% sequence identity with

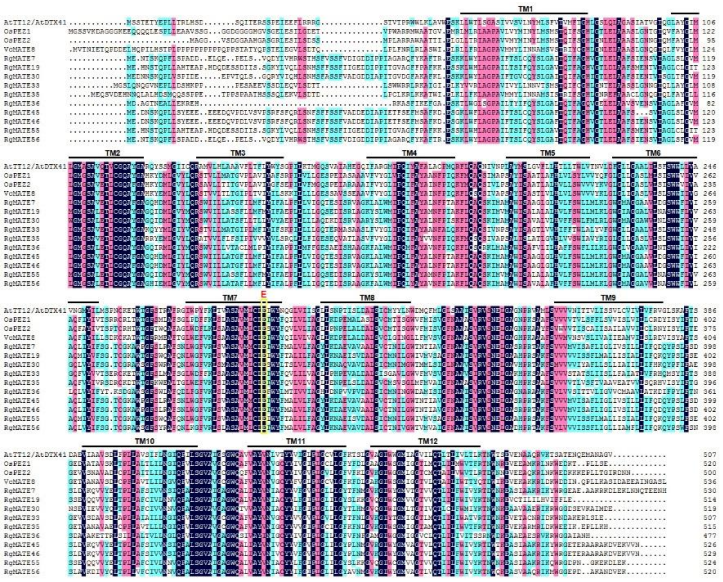

Fig. 3: Multiple sequence alignment of the deduced translation products of the set of the 10 *RgMATE*s with those of four heterologous MATEs implicated in the transport of phenolics. The predicted 12 transmembrane domains are indicated by underlining. The AtDTX41/AtTT12 E290 residue is highlighted by a yellow box

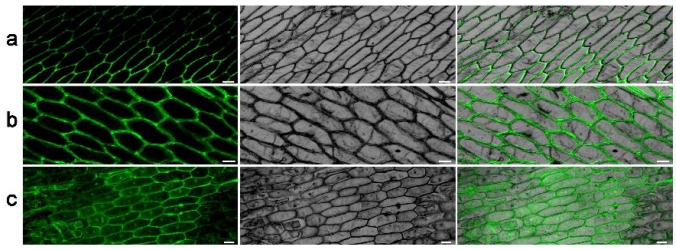

Fig. 4: Subcellular localization of the CaMV35S: GFP-RgMATEs fusion protein in onion epidermal cells. (a) CaMV35S:GFP-RgMATE33; (b) CaMV35S:GFP-RgMATE46; (c) CaMV35S:GFP (Bars = 100 µm)

the known MATEs (Table 3). In particular, RgMATE33 shared 47.4, 62.8, 63.7 and 69.5% identity with, respectively, AtDTX41/AtTT12, OsPEZ2, OsPEZ1 and VcMATE8. Some of the transmembrane domains conserved across the MATEs produced by *A. thaliana*, rice and blueberry were similarly conserved in *R. glutinosa* (Fig. 3); the sequence conservation extended to certain inter-transmembrane domain linkers, such as residue E290 in the inter-transmembrane 7 linker, which is critical for the functionality of AtDTX41/AtTT12. The equivalent residue featured in all of the 10 putative phenolics efflux transporting RgMATEs: E301 in RgMATE7, E306 in RgMATE19, E302 in RgMATE30, E292 in RgMATE33, E300 in RgMATE35, E265 in RgMATE36, E303 in RgMATE45, E307 in RgMATE46, E306 in RgMATE55 and E302 in RgMATE56. So we considered the 10 RgMATEs as phenolic efflux transport candidates for further analysis.

The subcellular localization of RgMATE33 and RgMATE46

Based on *in silico* localization analysis, we selected two (RgMATE33 and RgMATE46) of the RgMATE proteins to experimentally determine their subcellular localization. The two RgMATE complete coding regions were fused to the N-terminus of GFP and CaMV35S:RgMATE33-GFP and CaMV35S:RgMATE46-GFP constructs were transiently expressed in onion epidermal cells, respectively. The green fluorescence from fusion protein of CaMV35S:GFP-RgMATE33 and CaMV35S:GFP-RgMATE46 constructs were mainly both observed in the plasma membrane of the cells (Fig. 4a,b), while the expression of the control CaMV35S:GFP was detected in the cytoplasm, nucleus or other cell organelles (Fig. 4c). The results confirmed the *in silico* prediction of these RgMATE localization.

Phenolics accumulation of the root exudates

In the analysis of phenolics accumulation from hairy root exudates, total phenolics content from the root exudates exhibited an slight increase tendency during 5–20 days after transplant (DAT), then the phenolics accumulation of the exudates after 25 DAT was observed to be an obvious increase tendency. Among the nine time points,

Table 2: Characteristics of the deduced translation products of the RgMATE cDNAs

RgMATE ID	Amino acid number	Molecular mass (kDa)	pI	Instability index	Aliphatic index	GRAVY	TMD	Predicted localization
RgMATE1	484	52.87	6.07	28.26	116.67	0.68	12	plasma membrane
RgMATE2	535	58.57	5.38	29.99	110.92	0.62	12	plasma membrane
RgMATE3	530	57.90	5.52	28.12	112.13	0.68	12	plasma membrane
RgMATE4	534	58.63	5.13	32.61	109.46	0.61	12	plasma membrane
RgMATE5	502	54.72	4.98	29.98	114.48	0.76	12	plasma membrane
RgMATE6	524	57.28	5.29	31.20	112.46	0.69	12	vacuolar membrane
RgMATE7	530	58.19	7.00	30.47	112.11	0.61	12	plasma membrane
RgMATE8	510	55.28	6.92	26.97	120.86	0.76	10	plasma membrane
RgMATE9	498	54.61	6.65	27.79	116.67	0.67	10	plasma membrane
RgMATE10	502	54.99	7.05	32.54	121.57	0.71	10	plasma membrane
RgMATE11	481	52.92	8.64	34.28	119.83	0.70	9	plasma membrane
RgMATE12	512	55.10	8.59	29.78	114.96	0.63	9	vacuolar membrane
RgMATE13	496	54.74	5.84	27	111.27	0.67	10	plasma membrane
RgMATE14	524	58.07	7.56	30.62	117.56	0.55	11	plasma membrane
RgMATE15	480	52.83	8.64	33.93	120.08	0.70	9	plasma membrane
RgMATE16	535	58.57	5.50	29.83	111.64	0.63	12	plasma membrane
RgMATE17	523	57.01	8.28	35.51	122.47	0.79	10	endoplasmic reticulum
RgMATE18	486	53.49	8.21	22.56	120.74	0.81	10	plasma membrane
RgMATE19	514	56.33	5.98	31.63	120.31	0.82	12	plasma membrane
RgMATE20	546	58.51	8.72	32.19	109.23	0.45	10	plasma membrane
RgMATE21	535	58.51	5.38	29.44	110.52	0.63	12	plasma membrane
RgMATE22	535	58.52	5.36	29.23	109.63	0.63	12	plasma membrane
RgMATE23	537	58.92	5.27	30.46	110.32	0.60	12	plasma membrane
RgMATE24	536	58.76	5.25	29.49	109.24	0.61	12	plasma membrane
RgMATE25	535	58.80	5.27	29.03	109.81	0.63	12	plasma membrane
RgMATE26	535	58.56	5.40	29.99	110.36	0.61	12	plasma membrane
RgMATE27	484	52.87	6.07	28.26	116.67	0.68	12	plasma membrane
RgMATE28	480	52.11	7.97	31.63	121.19	0.72	12	plasma membrane
RgMATE29	488	52.87	5.91	24.72	114.49	0.67	12	plasma membrane
RgMATE30	519	57.33	6.39	30.29	115.76	0.70	12	plasma membrane
RgMATE31	490	53.70	5.80	27.78	120.00	0.71	10	plasma membrane
RgMATE32	489	53.94	8.69	35.95	123.64	0.69	11	plasma membrane
RgMATE33	507	54.99	6.09	24.89	118.84	0.69	12	plasma membrane
RgMATE34	484	52.87	6.07	28.26	116.67	0.68	12	plasma membrane
RgMATE35	515	56.15	7.06	28.08	118.66	0.64	12	plasma membrane
RgMATE36	477	51.73	6.95	32.43	120.48	0.83	10	plasma membrane
RgMATE37	491	53.60	6.53	28.62	119.74	0.70	12	plasma membrane
RgMATE38	506	55.56	5.84	30.91	116.98	0.67	11	plasma membrane
RgMATE39	584	62.43	9.19	37.52	107.05	0.50	9	plasma membrane
RgMATE40	510	55.37	6.21	26.07	117.98	0.72	11	plasma membrane
RgMATE41	532	58.36	5.49	28.60	111.33	0.62	10	plasma membrane
RgMATE42	470	50.56	5.99	27.34	122.62	0.78	10	plasma membrane
RgMATE43	502	54.82	7.01	30.30	115.16	0.72	12	plasma membrane
RgMATE44	484	52.89	6.07	28.42	116.88	0.68	12	plasma membrane
RgMATE45	526	57.68	5.30	30.50	112.21	0.68	12	plasma membrane
RgMATE46	529	58.01	5.20	30.80	112.31	0.67	12	plasma membrane
RgMATE47	495	54.14	7.60	30.30	112.73	0.64	10	plasma membrane
RgMATE48	490	52.75	5.99	27.49	122.59	0.77	12	plasma membrane
RgMATE49	570	62.64	8.56	41.51	111.21	0.39	11	plasma membrane
RgMATE50	485	52.99	8.97	24.55	117.13	0.66	10	plasma membrane
RgMATE51	535	58.57	5.38	29.99	110.92	0.62	12	plasma membrane
RgMATE52	486	53.55	6.33	39.93	118.91	0.70	10	nucleus
RgMATE53	479	52.62	6.98	30.18	116.05	0.65	10	plasma membrane
RgMATE54	490	52.78	5.99	27.66	121.80	0.76	12	plasma membrane
RgMATE55	524	57.41	6.70	30.16	115.25	0.67	12	plasma membrane
RgMATE56	520	57.25	8.05	28.69	112.77	0.69	12	plasma membrane
RgMATE57	516	56.36	5.31	27.31	115.50	0.69	10	plasma membrane
RgMATE58	484	52.87	6.07	28.26	116.67	0.68	12	plasma membrane
RgMATE59	510	55.75	8.28	32.87	119.88	0.75	9	plasma membrane
RgMATE60	537	58.91	5.37	30.10	109.39	0.60	10	plasma membrane
RgMATE61	502	54.68	6.52	29.81	119.10	0.73	11	plasma membrane
RgMATE62	477	52.59	5.76	31.74	113.10	0.63	12	plasma membrane
RgMATE63	501	54.70	7.02	26.82	115.95	0.68	12	plasma membrane
RgMATE64	510	55.35	6.21	28.01	118.75	0.73	11	plasma membrane
RgMATE65	478	52.42	7.56	27.79	115.42	0.75	9	plasma membrane
RgMATE66	484	52.87	6.07	28.26	116.67	0.68	12	plasma membrane

total phenolics content of the exudates was the highest at the 45 DAT (Fig. 5a). For example, total phenolics content of the root exudates at 45 DAT was approximately 15-fold relative to that at 10 DAT.

Expression profiles of the *RgMATEs* potentially involved in phenolics release

The expression abundance of *RgMATE33* was the highest among the ten genes (Fig. 5b). During the hairy roots-cultured stages, the expression abundance of *RgMATE33* mostly exhibited an increase tendency; the expression abundance of *RgMATE33* was the low at 5 DAT, while *RgMATE33* transcript was found most strongly expressed at 45 DAT, and followed by 40 DAT; The coefficients of determiantion (R^2) between *RgMATE33* expression abundance of the roots and the phenolics accumulation of their exudates were 0.979 (Table 4). *RgMATE7*, *RgMATE30*, *RgMATE35*, *RgMATE36*, *RgMATE46*, *RgMATE55* and *RgMATE56* largely exhibited a similar expression pattern with *RgMATE33*, and their R^2 values between the expression abundance and the phenolics accumulation were computed as more than 0.87. Compared with *RgMATE33*, the expression abundance of *RgMATE19* at 45 DAT was the lowest among various stages, its R^2 value between its expression abundance of the roots and the phenolics accumulation of the root exudates was very low ($R^2 = 0.257$). In addition, the expression abundance of *RgMATE45* was mostly no significant different at various time points, and the relevance between its expression abundance and the phenolics accumulation was even negative correlation. The expression profiles of the *RgMATEs* varied in various time points, which reflected potential different functions. Thus we speculated that the eight RgMATEs (including RgMATE7, RgMATE30, RgMATE33, RgMATE35, RgMATE36, RgMATE46, RgMATE55 and RgMATE56) could be related to the transport of phenolics release in *R. glutinosa* roots, while RgMATE19 and RgMATE45 might participate in other transport function.

Discussion

The roots of *R. glutinosa* produce pharmacologically active secondary metabolites, but some (especially phenolics) of these can also be secreted to plant rhizosphere and represent agents of auto toxic allelochemicals by inhibiting the uptake of nutrients when the species was continuously cultivated (Wu *et al*. 2015; Li *et al*. 2017). Members of the MATE family act to detoxify certain phenolics, in particular by their removal from the plant entirely (Omote *et al*. 2006; Chen *et al*. 2015). This property prompted the current interest in establishing the importance of MATEs in the release of phenolics from secondary metabolites. On the basis of a whole transcriptome, a set of *MATE* homologs was identified, with the intention of revealing which, if any, of these could be implicated in phenolics autotoxicity formation.

Table 3: The homology between 10 RgMATE candidaties and four known MATEs involved in the phenolics transport

RgMATE ID	Sequence identify (%)			
	AtDTX41/AtTT12	OsPEZ2	OsPEZ1	VcMATE8
RgMATE7	40.4	46.3	45.2	42.6
RgMATE19	40.0	45.1	45.1	40.9
RgMATE30	41.5	44.3	44.1	43.0
RgMATE33	47.4	62.8	63.7	69.5
RgMATE35	42.8	62.6	63.2	69.5
RgMATE36	42.6	48.0	45.8	42.3
RgMATE45	40.6	44.0	44.7	43.4
RgMATE46	40.8	44.3	44.9	43.6
RgMATE55	40.3	45.6	45.8	41.9
RgMATE56	40.5	43.9	45.0	43.4

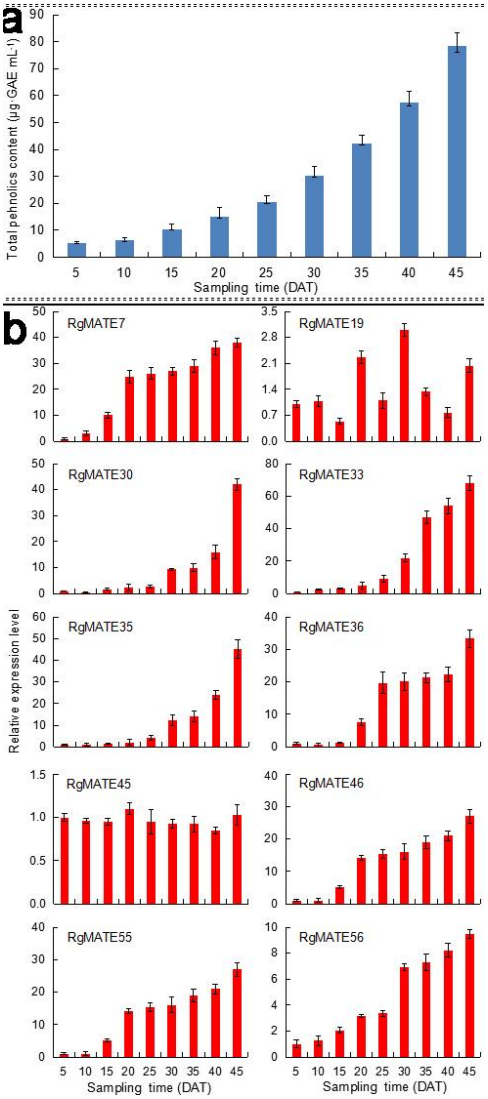

Fig. 5: (a) The accumulation of phenolics in *R. glutinosa* root exudates at various time points. (b) The temporal expression profiles of the 10 *RgMATEs* in *R. glutinosa* hairy roots by qRT-PCR experiment. The error bars represent the standard error (n =3)

Members of the MATE family range in length from ~400–700 residues, with the majority lying in the

Table 4: The correlation coefficient (R2) between the 10 *RgMATE* expression abundance (X variable) from *R. glutinosa* roots and total phenolics accumulation from their exduates (Y variable)

Sampling time	Y variable	Various X variables									
		RgMATE7	RgMATE19	RgMATE30	RgMATE33	RgMATE35	RgMATE36	RgMATE45	RgMATE46	RgMATE55	RgMATE56
5	3.3±0.56	1.00±0.23	1.00±0.09	1.00±0.12	1.00±0.23	1.00±0.27	1.00±0.33	1.00±0.04	1.00±0.27	1.00±0.31	1.00±0.24
10	4.3±1.01	3.09±0.89	1.09±0.14	0.41±0.24	2.34±0.24	1.01±0.47	0.21±0.47	0.96±0.03	1.03±0.65	1.26±0.37	1.31±0.37
15	7.04±2.09	10.11±1.23	0.54±0.07	1.59±0.37	3.32±0.33	1.52±0.28	1.20±0.14	0.95±0.04	5.17±0.34	2.07±0.22	8.55±0.36
20	15.23±3.24	20.85±2.45	2.26±0.17	2.4±0.55	5.19±0.56	2.02±0.56	7.57±0.99	1.11±0.07	14.21±0.75	3.17±0.14	10.55±1.45
25	20.34±2.45	22.05±3.56	1.1±0.21	2.69±0.46	8.95±1.04	4.08±0.98	19.72±3.24	0.95±0.14	15.43±1.34	3.36±0.23	16.64±2.34
30	30.24±3.43	27.15±2.89	3±0.17	9.31±0.98	22.04±2.37	12.3±2.34	20.09±2.79	0.92±0.05	16.05±2.37	6.93±0.24	24.14±2.47
35	42.35±2.97	28.98±2.47	1.35±0.11	10.01±1.45	46.97±3.78	14.09±2.47	21.32±1.56	0.92±0.09	19.02±1.98	7.31±0.67	26.51±1.98
40	57.38±4.36	36.00±2.57	0.78±0.13	15.99±2.75	54.06±4.89	24.02±2.01	22.29±2.12	0.85±0.04	20.98±1.49	8.23±0.53	27.62±1.76
45	78.34±5.14	38.02±2.96	2.04±0.19	42.03±2.24	68.15±4.35	44.98±4.25	33.31±2.68	1.03±0.12	27.09±2.01	9.45±0.34	29.31±2.56
R^2	-	0.871**	0.257	0.926**	0.979**	0.968**	0.924**	-0.190	0.919**	0.955**	0.902**

Mean ± standard deviation. "**" represents the significance level (P>0.01)

range 400–550 (Santos *et al*. 2017). The size distribution of the RgMATEs (470–584 residues) was consistent with this range (Chen *et al*. 2015). Most MATE proteins feature twelve transmembrane domains (Hvorup *et al*. 2003), but this number varies from eight to 14 among the MATEs produced by *A. thaliana* (Green and Rogers 2004). According to an *in silico* analysis, the number of transmembrane domains in *R. glutinosa* RgMATEs ranged from nine to twelve, suggesting that the RgMATEs possess typical transmembrane structure characteristics of transporters. Gene ontology revealed some aspects of the functionality of the RgMATEs (Ashburner *et al*. 2000). According to GO functional analysis, the RgMATEs were associated with membranes, were involved in transmembrane transporter and antiporter activity, and their primary functions included the detoxification and removal of toxins from the plant cell. The conclusion is that some of the RgMATEs could be involved in the release of endogenously produced toxins, acting to maintain cell function and cell membrane integrity.

The release of phenolics can enhance a plant's ability to absorb and utilize precipitated apoplasmic iron (Lu *et al*. 2018). Phylogenetic analyses of MATEs have been used to predict their substrate specificity (Liu *et al*. 2016; Wang *et al*. 2017a). The *R. glutinosa* RgMATEs formed four clades, indicative of a degree of functional diversity. Of C1 subfamily, the members of C1-1 included 33 of the RgMATEs, seven *A. thaliana* MATEs (AtDTX29 through 35) and seven heterologous sequences. AtDTX35 is known as a transporter which influences flavonoid content (Thompson *et al*. 2010), and VvAM1 involves in the transport of anthocyanins in the grapevine (Gomez *et al*. 2011). MtMATE2 mediates the vacuolar sequestration of flavonoid glycosides in barrel medic (Zhao *et al*. 2011), while NtJAT2 transports alkaloids in tobacco (Shitan *et al*. 2014). The members of C1-2 included 14 RgMATEs and nine *A. thaliana* MATEs (AtDTX20 through 28). Subgroup C1-3 clustered two of the RgMATEs, along with five *A. thaliana* MATEs (AtDTX36 through 40) and five heterologous sequences; most of these sequences have been associated with the release of phenolics (Ishimaru *et al*. 2011; Bashir *et al*. 2011; Chen *et al*. 2015). The C1-4 secondary clade harbored only a solitary *A. thaliana* member (AtDTX41/AtTT12), along with six heterologous sequences, all of which are involved in the transport or accumulation of flavonoids, anthocyanins and other phenolics into the plasma membrane or vacuole (Marinova *et al*. 2007; Chai *et al*. 2009; Frank *et al*. 2011; Chen *et al*. 2015; Yang *et al*. 2016). Thus we concluded that some of these RgMATEs belonging to C1 subfamily could be involved in phenolics transportation of *R. glutinosa*.

However, among the other three clades, the C2 clade clustered 12 of the RgMATEs, along with 19 *A. thaliana* MATEs (AtDTX1 through 19) and one tobacco protein (NtJAT1). AtDTX1 has relatively broad substrate specificity and confers tolerance to cadmium ions when expressed in *E. coli* (Li *et al*. 2002); AtDTX19/AtALF5 is transcribed in root epidermal cells, where it functions as a protectant against certain soil toxins (Diener *et al*. 2001). NtJAT1 participates in the sequestration of alkaloids within the vacuole and forms part of the plant response to pathogen attack (Morita *et al*. 2009). Subfamily C3 contained two RgMATEs in addition to nine *A. thaliana* MATEs (AtDTX48/AtZF14 through 56). AtDTX48/AtZF14 is involved in iron homeostasis during organ initiation and development (Wang *et al*. 2015), AtDTX51/AtADS1 negatively regulates disease resistance (Sun *et al*. 2011) and AtDTX56 localizes to the plasma membrane and participates in the response to an increased CO_2 concentration in the stomatal guard cells (Tian *et al*. 2015). Finally, the C4 clade harbored three of the RgMATEs, six *A. thaliana* MATEs (AtDTX42 through 47) and 11 heterologous sequences. AtDTX43/AtFRD3 is required for the expression of tolerance to excess zinc ions through its regulation of iron homeostasis (Roschzttardtz *et al*. 2011), while the soybean protein GmFRD3b is inducible by iron deficiency (Rogers *et al*. 2009). Some of the members of this clade act as citrate effluxers: these consist of the bread wheat protein TaMATE1B (Tovkach *et al*. 2013), the cereal rye proteins ScFRDL1 and ScFRDL2 (Yokosho *et al*. 2010), the barley protein HvAACT1 (Zhou *et al*. 2013), the rice proteins OsFDL1 and OsFRDL4 (Yokosho *et al*. 2009; 2011) and the *Eucalyptus camaldulensis* protein EcMATE1 (Sawaki *et al*. 2013). Thus we speculated that the RgMATEs

from the C2, C3 and C4 subfamilies could mostly play roles in *R. glutinosa* response to various stresses and other biological processes.

The inclusion in the analysis of heterologous MATEs of known specificity implied that some of the RgMATEs in C1 subfamily may well target phenolics, alkaloids and other toxic compounds. Thus, the rice proteins OsPEZ1 and OsPEZ2 have been shown to mediate the release of phenolics into the soil by stressed plants (Bashir *et al.* 2011; Ishimaru *et al*. 2011). In maize plants challenged by aluminum stress, MaMATE2 promoted the secretion of flavonoid-type phenolics from the roots (Maron *et al.* 2010). The blueberry protein VcMATE8 is also believed to function as a phenolic transporter (Chen *et al*. 2015). In all, ten of the RgMATEs were found to share at least 40% sequence similarity with four heterologous MATEs shown experimentally to mediate the transport of phenolics. The level of sequence conservation of certain of the (up to twelve) transmembrane domains present in the RgMATEs was quite high, and some inter-transmembrane linkers also appeared to be well conserved. It has been suggested that MATE proteins transport their "cargo" via a pore maintained by the transmembrane helices (Zhang *et al.* 2014), in which case maintaining the secondary structure of the relevant transmembrane domains is needed for a MATE to function (Wang *et al.* 2016). The *A. thaliana* MATE AtDTX41/AtTT12 is known to act as an anthocyanin transporter and/or a flavonoid/cation antiporter (Marinova *et al.* 2007); its E290 residue has been shown to be critical for both substrate transport (Marinova *et al*. 2007). Ten putative phenolics transporting RgMATEs all had the equivalent residue. Thus ten RgMATE transporters probably represent the candidates for the release of phenolics via the plasma membrane.

The subcellular localization of a transporter is crucial for its functionality. Majority of plant MATEs characterized to date are associated with either the plasma membrane or the vacuolar membrane (Chai *et al.* 2009; Shitan *et al.* 2014). Those localized to the plasma membrane mediate the efflux and detoxification from endogenous or exogenous toxins (Ishimaru *et al.* 2011; Miyauchi *et al.* 2017). Plant MATE characterized phenolics efflux transporters so far are localized to the plasma membrane and have a primary site for iron uptake (Xu *et al.* 2019; Wang *et al.* 2020). These MATE substrates are transported out of the cells in exchanges for the iron-influx (Jagessar *et al.* 2020). In rice, two MATEs (OsPEZ1 and OsPEZ1) were both localized to the plasma membrane and functioned as phenolics efflux transports with the involvement in Fe uptaking (Bashir *et al.* 2011; Ishimaru *et al.* 2011). Here, the overwhelming majority (94%) of the RgMATEs were predicted to act within the plasma membrane. The inference was that most of the RgMATEs are involved in extracellular secretory pathways used for the removal of toxins. To further analyze the potential function of the ten RgMATE candidates, RgMATE33 and RgMATE46 proteins by GFP fusion imaging were both verified to be localization in the plasma membrane. The results revealed that the prediction of the RgMATE subcelluar localization was fairly accurate. Thus the subcelluar localization of the RgMATEs by experimental confirmation further revealed the potential function of efflux transportation.

The amount of MATE transcript was closely related to transport the abundance of its substrates (Chen *et al.* 2015; Xu *et al.* 2019; Wang *et al.* 2020). In blueberry plants, the expression profiles of several *VcMATE* genes involved in phenolics transportation were closely coordinated with the anthocyanidins accumulation processes (Chen *et al.* 2015). In brown cotton, the expression of *GhTT12* as a proanthocyanidin transporter was positively connected with the substrate accumulation (Xu *et al.* 2019). Our study indicated that the eight *RgMATE* candidates exhibited similar temporal expression patterns, and their expression became stronger and stronger with the phenolics increase of *R. glutinosa* root exudates. Positive correlation between expression of the eight *RgMATE* genes (including *RgMATE7*, *RgMATE30*, *RgMATE35*, *RgMATE36*, *RgMATE46*, *RgMATE55* and *RgMATE56*) and the accumulation of phenolics in the root exudates reflected that they could be responsible for phenolics transports via the plasma membranes of *R. glutinosa* root cells. This implied that the eight RgMATE transporters could be the strongest candidates involved in phenolic release. It is possible therefore that a heightened activity of the RgMATEs could participate in phenolics release into the extracellular space, promoting the presence of phenolics in the root exudates.

Conclusion

Our study primarily identified 66 RgMATE transcripts in *R. glutinosa*. The *in silico* analysis and preliminary experimental evidence discovered eight RgMATE efflux transporter potentially involved in the release of phenolics. Although the function of the RgMATEs in details will need to verify by further experiments, our study revealed that they potentially acting as transporters could regulate phenolics release into the rhizosphere and thus are likely implicated in the accumulation of allelochemicals in *R. glutinosa*, laying the foundation for revealing the molecular basis of allelopathic autotoxicity formation.

Acknowledgements

This research was supported by grants from the National Natural Science Foundation of China (No. 81403037), the Key Research and Development Special Project of Henan Province (182102310606), the Science Foundation of Henan University of Technology (No. 2017RCJH05), the Program for Innovative Research Team (in Science and Technology) of the University of Henan Province (19IRTSTHN008) and the National Key Research and Development Program of China (2017YFC1700705).

Author Contributions

YYH performed the experiments and wrote the manuscript. YH and WCJ performed the experiments. LMJ, LRF, YYJ, ZZY and CD revised the manuscript. All authors have Read and approved the manuscript.

References

Ashburner M, CA Ball, JA Blake, D Botstein, H Butler, JM Cherry, AP Davis, K Dolinski, SS Dwight, JT Eppig, MA Harris, DP Hill, L Issel-Tarver, A Kasarskis, S Lewis, JC Matese, JE Richardson, M Ringwald, GM Rubin, G Sherlock (2000). Gene ontology: Tool for the unification of biology. *Nat Genet* 25:25–2910

Bashir K, Y Ishimaru, H Shimo, Y Kakei, T Senoura, R Takahashi, Y Sato, Y Sato, N Uozumi, H Nakanishi, NK Nishizawa (2011). Rice phenolics efflux transporter 2 (PEZ2) plays an important role in solubilizing apoplasmic iron. *Soil Sci Plant Nutr* 57:803–812

Chai Y, B Lei, H Huang, J Li, J Yin, Z Tang, R Wang, L Chen (2009). TRANSPARENT TESTA 12 genes from *Brassica napus* and parental species: Cloning, evolution, and diverential involvement in yellow seed trait. *Mol Genet Genomics* 281:109–123

Chen L, Y Liu, H Liu, L Kang, J Geng, Y Gai, Y Ding, H Sun, Y Li (2015). Identification and expression analysis of mate genes involved in flavonoid transport in blueberry plants. *PLoS One* 10; Atricle e0118578

Diener AC, RA Gaxiola, GR Fink (2001). *Arabidopsis* ALF5, a multidrug efflux transporter gene family member, confers resistance to toxins. *Plant Cell* 13:1625–1638

Frank S, M Keck, M Sagasser, K Niehaus, B Weisshaar, R Stracke (2011). Two differentially expressed MATE factor genes from apple complement the *Arabidopsis* transparent testa12 mutant. *Plant Biol* 13:42–50

Gomez C, G Conejero, L Torregrosa, V Cheynier, N Terrier, A Ageorges (2011). In vivo grapevine anthocyanin transport involves vesicle-mediated trafficking and the contribution of anthoMATE transporters and GST. *Plant J* 67:960–970

Green LS, EE Rogers (2004). FRD3 controls iron localization in *Arabidopsis*. *Plant Physiol* 136:2523–2531

Hvorup RN, B Winnen, AB Chang, Y Jiang, XF Zhou, MH Saier (2003). The multidrug/oligosaccharidyl-lipid/polysaccharide (MOP) exporter superfamily. *Eur J Biochem* 270:799–813

Ishimaru Y, Y Kakei, H Shimo, K Bashir, Y Sato, Y Sato, N Uozumi, H Nakanishi, NK Nishizawa (2011). A rice phenolic efflux transporter is essential for solubilizing precipitated apoplasmic iron in the plant stele. *J Biol Chem* 286:24649–24655

Jagessar KL, DP Claxton, RA Stein, HS Mchaourab (2020). Sequence and structural determinants of ligand-dependent alternating access of a MATE transporter. *Proc Natl Acad Sci USA* 117:4732–4740

Kim Y, J Son, YS Lee, J Wee, M Lee, K Cho (2020). Temperature-dependent competitive advantages of an allelopathic alga over non-allelopathic alga are altered by pollutants and initial algal abundance levels. *Sci Rep* 10; Article 4419

Kumar S, G Stecher, K Tamura (2016). MEGA7: Molecular evolutionary genetics analysis version 7.0 for bigger datasets. *Mol Biol Evol* 33:1870–1874

Li C, Y Liu, H Liu, L Kang, J Geng, Y Gai, Y Ding, H Sun, Y Li (2015). Identification and expression analysis of mate genes involved in flavonoid transport in blueberry plants. *PLoS One* 10; Article e0118578

Li L, Z He, GK Pandey, T Tsuchiya, S Luan (2002). Functional cloning and characterization of a plant efflux carrier for multidrug and heavy metal detoxification. *J Biol Chem* 277:5360–5368

Li M, Y Yang, F Feng, B Zhang, S Chen, C Yang, L Gu, F Wang, J Zhang, A Chen, W Lin, X Chen, Z Zhang (2017). Differential proteomic analysis of replanted *Rehmannia glutinosa* roots by iTRAQ reveals molecular mechanisms for formation of replant disease. *BMC Plant Biol* 17; Article 116

Li M, Y Yang, X Li, L Gu, F Wang, F Feng, Y Tian, F Wang, X Wang, W Lin, X Chen, Z Zhang (2015). Analysis of integrated multiple 'omics' datasets reveals the mechanisms of initiation and determination in the formation of tuberous roots in *Rehmannia glutinosa*. *J Exp Bot* 66:5837–5851

Li Y, S Dai, B Wang, Y Jiang, Y Ma, L Pan, K Wu, X Huang, J Zhang, Z Cai, J Zhao (2020). Autotoxic ginsenoside disrupts soil fungal microbiomes by stimulating potentially pathogenic microbes. *Appl. Environ. Microbiol* 86; Article e00130–20

Li Z, Y Yang, D Xie, L Zhu, Z Zhang, W Lin (2012). Identification of autotoxic compounds in fibrous roots of *Rehmannia* (*Rehmannia glutinosa Libosch*). *PLoS One* 7; Article e28806

Liu J, Y Li, W Wang, J Gai, Y Li (2016). Genome-wide analysis of MATE transporters and expression patterns of a subgroup of MATE genes in response to aluminum toxicity in soybean. *BMC Genomics* 17; Article 223

Livak KJ, TD Schmittgen (2001). Analysis of relative gene expression data using real-time quantitative PCR and the 2 (-Delta Delta C (T)). *Methods* 25:402–408

Lu P, RO Magwanga, XL Guo, JN Kirungu, H Lu, X Cai, Z Zhou, Y Wei, X Wang, Z Zhang, R Peng, K Wang, Y Wang (2018). Genome-wide analysis of multidrug and toxic compound extrusion (mate) family in *gossypium raimondii* and *gossypium arboreum* and its expression analysis under salt, cadmium, and drought stress. *G3* 8:2483–2500

Ma Q, R Yi, L Li, Z Liang, T Zeng, Y Zhang, H Huang, X Zhang, X Yin, Z Cai, Y Mu, Y Cheng, Q Zeng, X Li, H Nian (2018). GsMATE encoding a multidrug and toxic compound extrusion transporter enhances aluminum tolerance in *Arabidopsis thaliana*. *BMC Plant Biol* 18; Article 212

Marinova K, L Pourcel, B Weder, M Schwarz, D Barron, JM Routaboul, I Debeaujon, M Klein (2007). The *Arabidopsis* MATE transporter TT12 acts as a vacuolar flavonoid/H^+-antiporter active in proanthocyanidin-accumulating cells of the seed coat. *Plant Cell* 19:2023–2038

Maron LG, MA Pineros, CT Guimaraes, JV Magalhaes, JK Pleiman, C Mao, J Shaff, SN Belicuas, LV Kochian (2010). Two functionally distinct members of the MATE (multi-drug and toxic compound extrusion) family of transporters potentially underlie two major aluminum tolerance QTLs in maize. *Plant J* 61:728–740

Miyauchi H, S Moriyama, T Kusakizako, K Kumazaki, T Nakane, K Yamashita, K Hirata, N Dohmae, T Nishizawa, K Ito, T Miyaji, Y Moriyama, R Ishitani, O Nureki (2017). Structural basis for xenobiotic extrusion by eukaryotic MATE transporter. *Nat Commun* 8; Article 1633

Morita M, N Shitan, K Sawada, MCE Van Montagu, D Inze, H Rischer, A Goossens, KM Oksman-Caldentey, Y Moriyama, K Yazaki (2009). Vacuolar transport of nicotine is mediated by a multidrug and toxic compound extrusion (MATE) transporter in *Nicotiana tabacum*. *Proc Natl Acad Sci USA* 106:2447–2452

Moriyama Y, M Hiasa, T Matsumoto, H Omote (2008). Multidrug and toxic compound extrusion (MATE)-type proteins as anchor transporters for the excretion of metabolic waste products and xenobiotics. *Xenobiotica* 38:1107–1118

Murashige T, F Skoog (1962). A revised medium for rapid growth and bioassays with tobacco tissue cultures. *Physiol Plantarum* 15:473–497

Omote H, M Hiasa, T Matsumoto, M Otsuka, Y Moriyama (2006). The MATE proteinsas fundamental transporters of metabolic and xenobiotic organic cations. *Trend Pharmacol Sci* 27:587–593

Ren X, F He, Z Zhang, Q Yan, H Jin, Z Li, B Qin (2015). Isolation, identification, and autotoxicity effect of allelochemicals from rhizosphere soils of flue-cured tobacco. *J Agric Food Chem* 63:8975–8980

Rogers EE, X Wu, G Stacey, HT Nguyen (2009). Two MATE proteins play a role in iron efficiency in soybean. *J Plant Physiol* 166:1453–1459

Roschzttardtz H, M Seguela-Arnaud, JF Briat, G Vert, C Curie (2011). The FRD3 citrate effluxer promotes iron nutrition between symplastically disconnected tissues throughout *Arabidopsis* development. *Plant Cell* 23:2725–2737

Saier MH, VS Reddy, BV Tsu, MS Ahmed, C Li, G Moreno-Hagelsieb (2016). The transporter classification database (TCDB): Recent advances. *Nucl Acids Res* 44:D372–D379

Santos ALD, S Chaves-Silva, L Yang, LGS Maia, A Chalfun-Júnior, S Sinharoy, J Zhao, VA Benedito (2017). Global analysis of the MATE gene family of metabolite transporters in tomato. *BMC Plant Biol* 17; Article 185

Bursal E, İ Gülçin (2011). Polyphenol contents and in vitro antioxidant activities of lyophilised aqueous extract of kiwifruit (*Actinidia deliciosa*). *Food Res Intl* 44:1482–1489

Sawaki Y, T Kihara-Doi, Y Kobayashi, N Nishikubo, T Kawazu, H Koyama, S Sato (2013). Characterization of Al-responsive citrate excretion and citrate-transporting MATEs in *Eucalyptus camaldulensis*. *Planta* 237:979–989

Shitan N, S Minami, M Morita, M Hayashida, S Ito, K Takanashi, H Omote, Y Moriyama, A Sugiyama, A Goossens, M Moriyasu, K Yazaki (2014). Involvement of the leaf-specific multidrug and toxic compound extrusion (MATE) transporter Nt-JAT2 in vacuolar sequestration of nicotine in *Nicotiana tabacum*. *PLoS One* 9; Article e108789

Sun X, EM Gilroy, A Chini, PL Nurmberg, I Hein, C Lacomme, PR Birch, A Hussain, BW Yun, GJ Loake (2011). ADS1 encodes a MATE-transporter that negatively regulates plant disease resistance. *New Phytol* 192:471–482

Thompson EP, C Wilkins, V Demidchik, JM Davies, BJ Glover (2010). An *Arabidopsis* flavonoid transporter is required for anther dehiscence and pollen development. *J Exp Bot* 61:439–451

Tian W, CC Hou, ZJ Ren, YJ Pan, JJ Jia, HW Zhang, FL Bai, P Zhang, HF Zhu, YK He, SL Luo, LG Li, S Luan (2015). A molecular pathway for CO_2 response in *Arabidopsis* guard cells. *Nat Commun* 6; Article 6057

Tian Y, Q Wang, W Zhang, L Gao (2016). Reducing environmental risk of excessively fertilized soils and improving cucumber growth by *Caragana* microphylla-straw compost application in long-term continuous cropping systems. *Sci Total Environ* 544:251–261

Tiwari M, D Sharma, M Singh, RD Tripathi, PK Trivedi (2014). Expression of OsMATE1 and OsMATE2 alters development, stress responses and pathogen susceptibility in *Arabidopsis*. *Sci Rep* 4; Article 3964

Tovkach A, PR Ryan, AE Richardson, DC Lewis, TM Rathjen, S Ramesh, SD Tyerman, E Delhaize (2013). Transposon-mediated alteration of TaMATE1B expression in wheat confers constitutive citrate efflux from root apices. *Plant Physiol* 161:880–892

Wang FQ, JY Zhi, ZY Zhang, LN Wang, YF Suo, CX Xie, MJ Li, B Zhang, JF Du, L Gu, HZ Sun (2017b). Transcriptome analysis of salicylic acid treatment in *Rehmannia glutinosa* hairy roots using RNA-seq technique for identification of genes involved in acteoside biosynthesis. *Front Plant Sci* 8; Article 787

Wang J, Q Hou, P Li, L Yang, X Sun, VA Benedito, JQ Wen, B Chen, KS Mysore, J Zhao (2017a). Diverse functions of multidrug and toxin extrusion (MATE) transporters in citric acid efflux and metal homeostasis in *Medicago truncatula*. *Plant J* 90:79–95

Wang L, X Bei, J Gao, Y Li, Y Yan, Y Hu (2016). The similar and different evolutionary trends of MATE family occurred between rice and *Arabidopsis thaliana*. *BMC Plant Biol* 16; Article 207

Wang R, X Liu, S Liang, Q Ge, Y Li, J Shao, Y Qi, L An, F Yu (2015). A subgroup of MATE transporter genes regulates hypocotyl cell elongation in *Arabidopsis*. *J Exp Bot* 66:6327–6343

Wang Y, W Yu, Y Cao, Y Cai, S Lyi, W Wu, Y Kang, C Liang, J Liu (2020). An exclusion mechanism is epistatic to an internal detoxification mechanism in aluminum resistance in *Arabidopsis*. *BMC Plant Biol* 20; Article 122

Wise AA, Z Liu, AN Binns (2006). Three methods for the introduction of foreign DNA into *Agrobacterium*. *Methods Mol Biol* 343:43–54

Wu L, J Wang, W Huang, H Wu, J Chen, Y Yang, Z Zhang, W Lin (2015). Plant-microbe rhizosphere interactions mediated by *Rehmannia glutinosa* root exudates under consecutive monoculture. *Sci Rep* 5; Article 15871

Xu L, ZL Shen, W Chen, GY Si, Y Meng, N Guo, X Sun, YP Cai, Y Lin, JS Gao (2019). Phylogenetic analysis of upland cotton MATE gene family reveals a conserved subfamily involved in transport of proanthocyanidins. *Mol Biol Rep* 46:161–175

Yang SC, Y Jiang, LQ Xu, K Shiratake, ZR Luo, QL Zhang (2016). Molecular cloning and functional characterization of DkMATE1 involved in proanthocyanidin precursor transport in persimmon (*Diospyros kaki* Thunb.) fruit. *Plant Physiol Biochem* 108:241–250

Yokosho K, N Yamaji, D Ueno, N Mitani, JF Ma (2009). OsFRDL1 is a citrate transporter required for efficient translocation of iron in rice. *Plant Physiol* 149:297–305

Yokosho K, N Yamaji, JF Ma (2010). Isolation and characterisation of two MATE genes in rye. *Funct Plant Biol* 37:296–303

Yokosho K, N Yamaji, JF Ma (2011). An Al-inducible MATE gene is involved in external detoxification of Al in rice. *Plant J* 68:1061–1069

Zhang B, X Li, L Zhang, L Gu, F Feng, M Li, F Wang, W Lin, Z Zhang (2018). Alleviatory effect of spent Pl*eurotus eryngii* quel substrate on replant problem of *Rehmannia glutinosa* Libosch. *Intl J Phytoremediat* 20:61–67

Zhang B, XZ Li, FQ Wang, MJ Li, JY Zhang, L Gu, LJ Zhang, WQ Tu, ZY Zhang (2016). Assaying the potential autotoxins and microbial community associated with *Rehmannia glutinosa*, replant problems based on its 'autotoxic circle'. *Plant Soil* 407:307–322

Zhang H, H Zhu, Y Pan, Y Yu, S Luan, L Li (2014). A DTX/MATE-type transporter facilitates abscisic acid efflux and modulates ABA sensitivity and drought tolerance in *Arabidopsis*. *Mol Plant* 7:1522–1532

Zhao J, D Huhman, G Shadle, X He, LW Sumner, Y Tang, RA Dixon (2011). MATE2 mediates vacuolar sequestration of flavonoid glycosides and glycoside malonates in *Medicago truncatula*. *Plant Cell* 23:1536–1555

Zhao J, RA Dixon (2009). MATE transporters facilitate vacuolar uptake of epicatechin 3′-O-glucoside for proanthocyanidin biosynthesis in *Medicago truncatul*a and *Arabidopsis*. *Plant Cell* 21:2323–2340

Zhou G, E Delhaize, M Zhou, PR Ryan (2013). The barley MATE gene, HvAACT1, increases citrate efflux and Al^{3+} tolerance when expressed in wheat and barley. *Ann Bot* 112:603–612